



STARCASTING

BY S. BUSINGER, R. McLAREN, R. OGASAWARA,
D. SIMONS, AND R. J. WAINSCOAT

The summit of Mauna Kea¹ on the Island of Hawaii is widely recognized as a premier site for ground-based astronomy. Mauna Kea Observatories, the world's largest astronomical observatory complex, comprises 13 telescopes, including the 2 Keck telescopes, the largest optical/infrared tele-

scopes in the world, and the newly operational Gemini North and Subaru telescopes (Fig. 1). Much of the uniqueness of this site is owed to its remote subtropical location in the northeastern Pacific Ocean and a summit area altitude of ~4200 m (nearly 14,000 ft). At ~20° latitude, Mauna Kea is in a region of cloud-suppressing subsidence associated with a prevailing Hadley cell in the central North Pacific.

¹ "White Mountain" in Hawaiian.

School of Ocean and Earth Science and Technology Contribution Number 5979.

AFFILIATIONS: BUSINGER—Department of Meteorology, University of Hawaii at Manoa, Honolulu, Hawaii; McLAREN AND WAINSCOAT—Institute for Astronomy, University of Hawaii at Manoa, Honolulu, Hawaii; OGASAWARA—Subaru Telescope, Hilo, Hawaii; SIMONS—Gemini Observatory, Hilo, Hawaii

CORRESPONDING AUTHOR: Professor Steven Businger, Department of Meteorology, University of Hawaii at Manoa, 2525 Correa Road, Honolulu, HI 96822
E-mail: businger@soest.hawaii.edu

In final form 8 March 2002
© 2002 American Meteorological Society

Moreover, telescopes here can view a large portion of the sky over both the Northern and Southern Hemispheres. The summit usually lies well above the persistent trade wind inversion that traps most cloudiness, water vapor, and pollutants within 1,500–3,000 m of sea level (Grinding 1992) and maintains strong atmospheric stability (Fig. 2, top). Only ~60% of the mass of the atmosphere and, on average, ~5% of the water vapor lie above the summit. Isolation from large population centers results in minimal aerosol content overhead and, combined with an

librium. Thus, accurate predictions of the summit air temperature at sunset and the change of temperature during the night are needed to achieve desired thermal equilibrium.

Moderately strong winds at the summit affect telescope tracking and result in wind shake. Moreover, wind-blown dust deposited on the telescope mirrors can reduce mirror reflectivity and increase emissivity in the infrared, and may cause telescope mirror damage. By performing observations in the downwind direction, image degradation from telescope

A new operational and research project at the University of Hawaii specializes in custom forecasting fair weather factors of astronomical interest, such as turbidity, scintillation, and others, to help observatory researchers maximize Mauna Kea's valuable telescope resources.

islandwide lighting ordinance, ensures a very dark nighttime sky. The remote island location and gentle slope of the volcano contribute to a relatively low atmospheric turbulence in the free atmosphere above the summit and this in turn leads to a very low level of atmospheric distortion in astronomical images. As a result of these many factors, the atmosphere above Mauna Kea most often is clear, clean, dry, and nearly transparent at optical and infrared window wavelengths (Morrison et al. 1973; Erasmus 1986). In addition to favorable weather conditions, the relatively shallow slope of this massive shield volcano and the absence of permanent snow make the summit easily accessible by road.

While weather conditions at Mauna Kea Observatories are generally favorable, there is substantial variability due to changing synoptic-scale weather systems and embedded mesoscale circulations in a region of complex terrain. Even during prevailing clear-sky periods, atmospheric variability strongly influences the success of astronomical operations (Roddier et al. 1990). This variability is produced by the degree of turbulence in the free atmosphere above the summit, the magnitude of frictionally induced turbulence in the summit boundary layer, and temperature variability inside and around the telescope domes.

Telescope and dome environments, in particular the primary mirror, must be maintained at a temperature within 1°C of the ambient outside temperature for optimum image quality. Large temperature differences result in image degradation caused by heat fluxes between the mirror and overlying air. Telescope primary mirrors have large thermal mass and many hours are needed to achieve thermal equi-

librium. Accurate summit wind forecasts benefit decisions regarding the pointing of telescope domes, which in turn determine which astronomical objects can be observed.

The transmissivity of infrared radiation depends upon the atmospheric moisture content above the summit. Water vapor in the earth's atmosphere strongly limits astronomical observations at wavelengths between 1 μm and 1 mm. Integrated precipitable water vapor (IPWV) is the variable typically monitored by ground-based astronomers observing at infrared and submillimeter wavelengths since it describes the total water vapor content above a particular altitude. Observations at wavelengths longer than 5 μm are productive only during periods of unusually low IPWV (<1 mm over Mauna Kea). Consequently, IPWV predictions can be used to set priorities for infrared and submillimeter observing programs. Nowcasts and forecasts of the fraction of sky covered by clouds over Mauna Kea allow selection between optical spectroscopic programs, which do not rely on absolute photometric calibration, and programs that do rely on good photometric conditions.

Adverse weather conditions. Snowfall and ice present significant hazards for transportation when they accumulate on the summit access road. During clear periods, the surface of the summit road radiatively cools to a temperature several degrees below the free atmosphere's temperature at night. Subsequent upslope advection of moisture during the night can result in a rapid buildup of black ice on the summit



FIG. 1. Photo of the summit of Mauna Kea viewed from the northeast. In the foreground on the summit ridge, from left to right, are the University of Hawaii (UH) 0.6-m telescope (small white dome), the United Kingdom Infrared Telescope, the UH 2.2-m telescope, the Gemini North 8-m telescope (silver, open), and the Canada–France–Hawaii Telescope. On the right are the NASA Infrared Telescope Facility (silver), the twin domes of the W. M. Keck Observatory; behind and to the left of them is the Subaru Telescope. In the valley below are the Caltech Submillimeter Observatory (silver), the James Clerk Maxwell Telescope (white, open), and the assembly building for the submillimeter array. The cinder cone in the center of the photograph is Pu‘u Poliahu. In the distance is the dormant volcano Hualalai (altitude 2,520 m), located near Kailua-Kona. (Photograph by Richard Wainscoat.)

access road, producing very hazardous driving conditions.

Synoptic-scale weather systems responsible for adverse weather conditions can occur at any time of year but are most common during the cool season (Kodama and Businger 1998). The midlatitude storm track over the northern Pacific is active in winter and causes an average of nine cold frontal passages across the Island of Hawaii per year (Worthley 1967). High winds, fog, icing, and snowfall generally accompany frontal passages. Snowfall totals from individual storms usually range from 2 to 7 cm. Less frequently, significant snowfalls can prevent access to the summit for several days (Fig. 2, bottom).

Upper-level troughs that form in the vicinity of the islands produce extensive cloud systems (Fig. 3a). Occasionally a stronger upper-level low will cut off from the westerlies and induce a low pressure system that extends to sea level near Hawaii (Fig. 3b). These subtropical cyclones or kona lows occur during the cool season and can cause blizzard conditions at the summit, with severe thunderstorms and flash floods



FIG. 2. (top) A convective cloud rises up the sun-warmed slopes of Mauna Loa and low clouds below a trade wind inversion. Photo taken from the south slope of Mauna Kea. (bottom) View of the Mauna Kea summit road with snow and ice approaching the domes of the University of Hawaii 24" (0.6 m) telescope (left) and the United Kingdom Infrared Telescope (right) taken in 1979. (Photo courtesy of the Institute for Astronomy.)

at lower altitudes (Fig. 2, bottom; Businger et al. 1998; Morrison and Businger 2001).

Strong summit winds can also occur during clear periods when strong anticyclones form north of Hawaii (Mello 1998). As summit wind speeds increase, working conditions become increasingly hazardous inside the dome, and observing is usually discontinued at wind speeds $>25 \text{ m s}^{-1}$. Driving on the access road and outside maintenance projects are also halted during periods of very strong winds, particularly in winter when the summit wind chill factor can be $<-45^\circ\text{C}$.

Tropical cyclones can occur over the central North Pacific Ocean during the summer and fall (Kodama and Businger 1998). Most of these cyclones either pass to the south of Hawaii or dissipate well to the east of the state, most commonly victims of wind shear. However, Hurricane Iniki, which struck Kauai in September 1992, highlights the potential danger of a similar impact on the Island of Hawaii in the future.

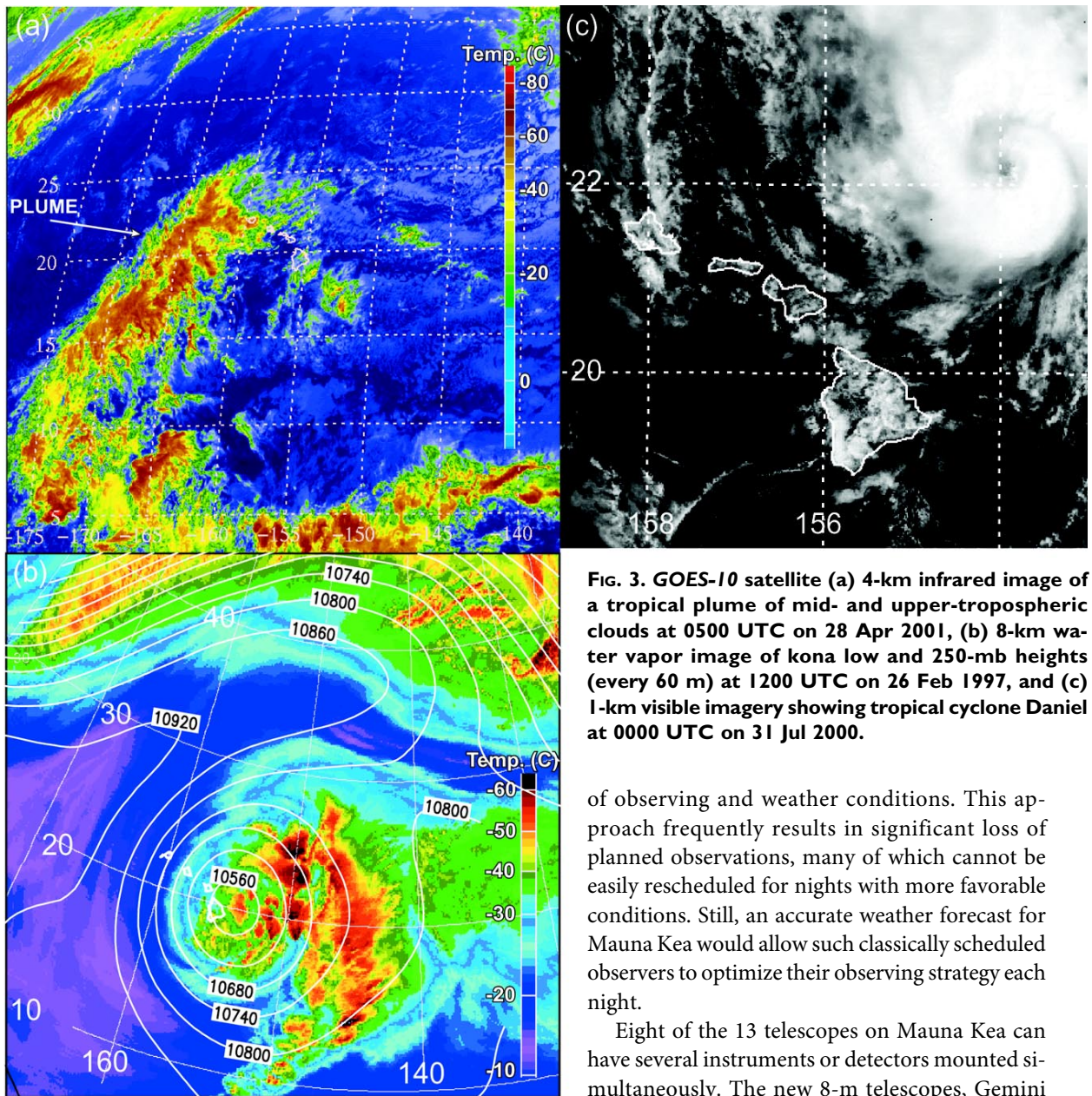


FIG. 3. GOES-10 satellite (a) 4-km infrared image of a tropical plume of mid- and upper-tropospheric clouds at 0500 UTC on 28 Apr 2001, (b) 8-km water vapor image of kona low and 250-mb heights (every 60 m) at 1200 UTC on 26 Feb 1997, and (c) 1-km visible imagery showing tropical cyclone Daniel at 0000 UTC on 31 Jul 2000.

Tropical cyclone landfall has not occurred on the Island of Hawaii during the past several decades. Despite this fortunate history, tropical cyclones can indirectly affect Mauna Kea. For example, tropical cyclone Daniel passed approximately 250 km north of Mauna Kea on 31 July 2000, disrupting the trade wind inversion, which caused thunderstorms (lightning strikes lead to power outages at the observatories) and an extended period of summit fog (Fig. 3c).

Observing strategies and telescope scheduling. For most of the last century, telescopes have had a fixed observation schedule for a particular night that is followed regardless

of observing and weather conditions. This approach frequently results in significant loss of planned observations, many of which cannot be easily rescheduled for nights with more favorable conditions. Still, an accurate weather forecast for Mauna Kea would allow such classically scheduled observers to optimize their observing strategy each night.

Eight of the 13 telescopes on Mauna Kea can have several instruments or detectors mounted simultaneously. The new 8-m telescopes, Gemini North and Subaru, both have multiple instruments available for rapid instrument changes (Fig. 4). This flexible-instrument technology permits observations to be tailored to take best advantage of the weather conditions each night. For example, on a night with low water vapor content in the atmosphere, but relatively large turbulence, optimum observations are in the midinfrared. As the turbulence decreases, conditions favor optical observations.

Several telescopes at Mauna Kea are currently experimenting with “queue scheduling,” and the Gemini Observatory schedules approximately half of its observing time in queue mode. This approach allows support staff to schedule the observations

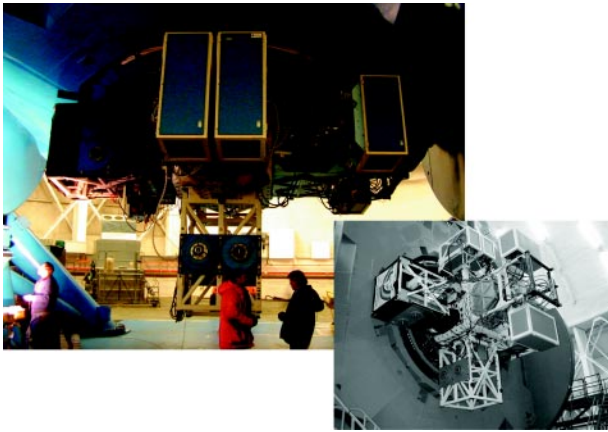


FIG. 4. Instrument mount on the Gemini North telescope showing multiple instrument capacity (Photographs by Peter Michaud).

in a manner that makes best use of the conditions. Queue scheduling can trigger changes in the type of observations done, the instrument in use on the telescope, or both. Observations that are prevented by adverse weather are also more easily rescheduled.

The image quality of large ground-based optical/near-infrared telescopes is limited by dynamic atmospheric turbulence above the telescope and inside the dome, and second, by quasi-static errors in the telescope itself. Adaptive optics is used to mitigate the first limitation, and active optics is used to mitigate the second, ultimately giving images near the diffraction limit of the primary mirror. There are a number of physical limitations to adaptive optics performance, leading to successive generations of more and more sophisticated techniques. Advance knowledge of the vertical location and strength of enhanced turbulence can be used to tune adaptive optics procedures. The impact of adaptive optics is readily apparent in Fig. 5.

Remote observing is becoming increasingly common at Mauna Kea and has been facilitated by improvements in high-bandwidth communication. Three telescopes on Mauna Kea (Keck 1, Keck 2, and the UH 0.6 m) are operated remotely on a routine basis. Since remote telescope operators cannot walk outside the dome to see the weather conditions, frequently updated satellite images with fine spatial resolution are valuable in discerning the presence of water vapor, liquid water droplets, and ice crystals located above the summit. Knowledge of the presence of any cloud cover is critical to photometry.

Recent studies have shown some feasibility for forecasts having sufficient accuracy to be incorporated into the flexible ground-based astronomy operations just described. Several case studies of various approaches to forecasting turbulence and a variable

called seeing (see the section, “Forecasting Observing Quality—Seeing Parameters” for a description) have been conducted during the last two decades (e.g., Coulman et al. 1986; Bougeault et al. 1995; Masciadri et al. 1998; Jumper and Beland 2000). Erasmus and Peterson (1997) describe the skill in operational forecasts of cirrus and precipitable water that are currently issued for the European Southern Observatories’ telescopes in northern Chile.

The recent innovations in telescope instrumentation, coupled with progress in mesoscale numerical prediction, have made an imperative case for investment in custom weather forecast support for Mauna Kea. The Mauna Kea Weather Center (MKWC) was established in July 1998 at the University of Hawaii at Manoa, with the following principal objectives: (i) to provide custom weather forecasts and nowcasts for the Mauna Kea Observatories, (ii) to acquire specific expertise regarding the weather conditions that provide for the best astronomical observing conditions with the aim of better anticipating these conditions, (iii) to develop an operational mesoscale modeling capability focused on forecasting atmospheric optical properties above the summit, and (iv) to provide an efficient mechanism to communicate forecast and meteorological data to the participating observatories. This paper describes the research challenges and the operational activities implemented during the first two years of the MKWC to address these objectives.

CUSTOM FORECASTING FOR MAUNA KEA.

The Mauna Kea Weather Center resides in the Department of Meteorology at the University of Ha-

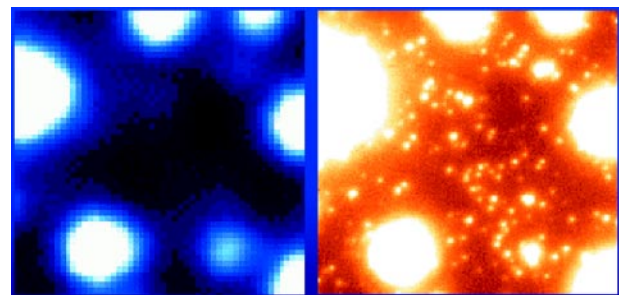


FIG. 5. These two images show the same small region, approximately $5'' \times 5''$, of the core of the globular cluster M13. The image on the right was taken with Hokupaa on the Gemini North telescope at $2.2 \mu\text{m}$, with an integration time of 940 s, and is corrected by adaptive optics, demonstrating the power of the telescope with adaptive optics to resolve and detect the many individual faint stars. For comparison, the image on the left shows the corresponding field in a short exposure image at visible wavelengths ($0.55 \mu\text{m}$) taken with the Gemini acquisition camera. See text for further explanation.

waii at Manoa in Honolulu and utilizes a growing suite of computational resources distributed across two islands (Fig. 6). Since January 1999, the MKWC has issued custom weather forecasts for the Mauna Kea Observatories twice daily, Monday through Friday. Forecast variables are specified at 6–12-h intervals out to 72 h, and extended outlooks provide an overview of general weather conditions 4–7 days ahead. The content of the forecasts has gradually evolved during the first two years of the project.

The MKWC Web site (hokukea.soest.hawaii.edu) is the primary means by which custom forecasts, satellite data, model output, and summit weather observations are made available to the astronomy community. The Web server locally generates global model and satellite graphics from gridded model output and digital satellite data. A second workstation generates additional satellite and model graphics for the Web site. A 400-GB RAID disk drive archive system attached to this workstation stores operational in situ data, satellite data, and model output for easy access, prior to archival to tape. This disk archive allows for efficient online access to a long period of data for case studies. A third workstation ingests data from the National Weather Service Forecast Office–Honolulu Forecast Office (NWSFO–HFO),² which is located in the same building as the Department of Meteorology. Close collaboration between the NWSFO–HFO and the MKWC ensures timely delivery of NWS advisories and warnings and efficient access to the NWS data stream. Additionally, workstations and a supercomputer in Hilo on the Island of Hawaii are utilized in an operational mesoscale modeling effort dedicated to MKWC forecasting and research (Fig. 6).

The MKWC utilizes forecast guidance from a combination of global models from national operational centers and from a local, dedicated mesoscale numerical modeling effort. The primary global model used is the National Centers for Environmental Prediction’s (NCEP) Aviation Model (AVN). This spectral model’s resolution near Hawaii is ~80 km. This relatively coarse grid spacing does not resolve the terrain of the Hawaiian Islands. Therefore, the AVN cannot provide explicit prognoses for conditions at the Mauna Kea summit. However, the AVN provides useful guidance for the 24–72 h forecast period, and output from NCEP’s Medium-Range Forecast (MRF) model is used in preparing extended outlooks out to seven days.

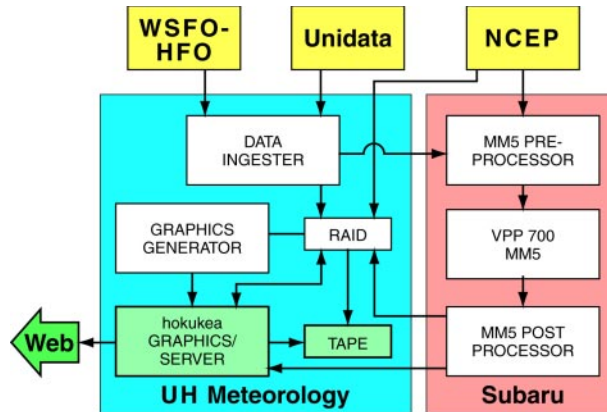


Fig. 6. Schematic of the distribution of computational and data resources utilized by the MKWC. Boxes designated MM5 refer to MM5 functions.

The mesoscale numerical model used at the MKWC is version 3 of the fifth-generation Pennsylvania State University–National Center for Atmospheric Research (Penn State–NCAR) Mesoscale Model (MM5; Grell et al. 1995), with extensions for running on distributed memory, message-passing parallel computers (Michalakes 1998). Since July 1999, a 42-h MM5 simulation utilizing four two-way nested domains has been running once daily on 16 vector processors of a Fujitsu VPP 700 that is located at the Subaru Telescope supercomputer facility in Hilo. The finest horizontal grid spacing is 1 km over Mauna Kea, enabling representation of the summit altitude to within ~175 m (Fig. 7). Forty-two sigma levels are used in the vertical, with the top level at 10 hPa. The terrain-following levels are more closely spaced near the ground. Over the Mauna Kea summit, the vertical grid spacing is approximately 15 m in the lowest 100 m and gradually increases to ~250 m in the upper troposphere.

The Subaru supercomputer facility provides dedicated access to three machines to handle all major phases of the daily MM5 simulations (pre- and post-processing; Fig. 6). The MM5 process is fully automated but requires significant attention and is continuously under development. The initial time for the MM5 runs is 0000 UTC [1400 Hawaiian standard time (HST)]. Initial conditions for all four domains and boundary conditions for the outermost domain are derived from the 0000 UTC AVN global model run. Work has begun toward utilizing the Local Analysis and Prediction System (LAPS; Birkenheuer 1999) to assimilate local in situ and satellite data. Preprocessing of the MM5 grids is completed by 0700 UTC (2100 HST). The simulation is completed in approximately 8 h, providing output by 1500 UTC

² The NWSFO–HFO is collocated with the MKWC in the Hawaii Institute of Geophysics Building at the University of Hawaii at Manoa.

(0500 HST). Graphical output is produced during the actual simulation, as each hour of model output becomes available, and it is completed and available to the MKWC forecaster by about 1700 UTC (0700 HST) for the morning forecast issued at 2000 UTC (1000 HST).

The MM5 simulations are nonhydrostatic and employ a comprehensive physics package. The explicit (grid resolvable) Reisner moisture scheme allows for mixed phase, whereby water and ice can exist simultaneously. The Grell (1993) cumulus parameterization is used in domains 1 and 2 (Fig. 7). Also included are the parameterization of shallow convection, a high-resolution MRF boundary layer, and longwave and shortwave radiation interactions with water vapor, clouds, precipitation, and the surface. The effects of both dry and moist vertical diffusion are included, and a first-order turbulence closure scheme is used.

The latest model graphics generated from the MM5, AVN, and MRF operational model output are posted on the MKWC Web site as output becomes available.

The Web interface provides for convenient comparison of graphical output across consecutive model runs.

In situ and satellite data. Hawaii and the Mauna Kea Observatories lie within a large data-sparse maritime environment. As a consequence, the availability of in situ data is limited. Only two conventional radiosondes are released from the Hawaiian Islands at 0000 and 1200 UTC daily. The nearest radiosonde site to Mauna Kea is Hilo, Hawaii, located near sea level about 50 km southeast of Mauna Kea. Data from this radiosonde site are useful for measuring upper-tropospheric winds, the freezing level, and the location and strength of the temperature inversion, but moisture data for deriving precipitable water above summit altitude are not consistently reliable. Moreover, the vertical resolution of the profile is too coarse to accurately parameterize turbulence and calculate seeing (refer to the section “Forecasting Observing Quality—Seeing Parameters for details), although a general estimate is possible based upon the

wind profile. A second radiosonde site is located at Lihue on Kauai, ~500 km northwest of Mauna Kea. Approximately 30 surface reporting stations are scattered throughout the island chain, 7 of which are located on the Island of Hawaii. Several other surface stations collect data that are not transmitted in real time.

Weather observations are routinely collected at the summit of Mauna Kea; however, no routine measurements of snowfall or snow depth are collected. The Canada–France–Hawaii Telescope (CFHT), the United Kingdom Infrared Telescope (UKIRT), the James Clerk Maxwell Telescope (JCMT), and the Subaru Telescope (Fig. 1) all operate weather towers with instrumentation located between 5 and 15 m above the ground. Each tower reports wind speed and direction, relative humidity, temperature, and pressure every 5–

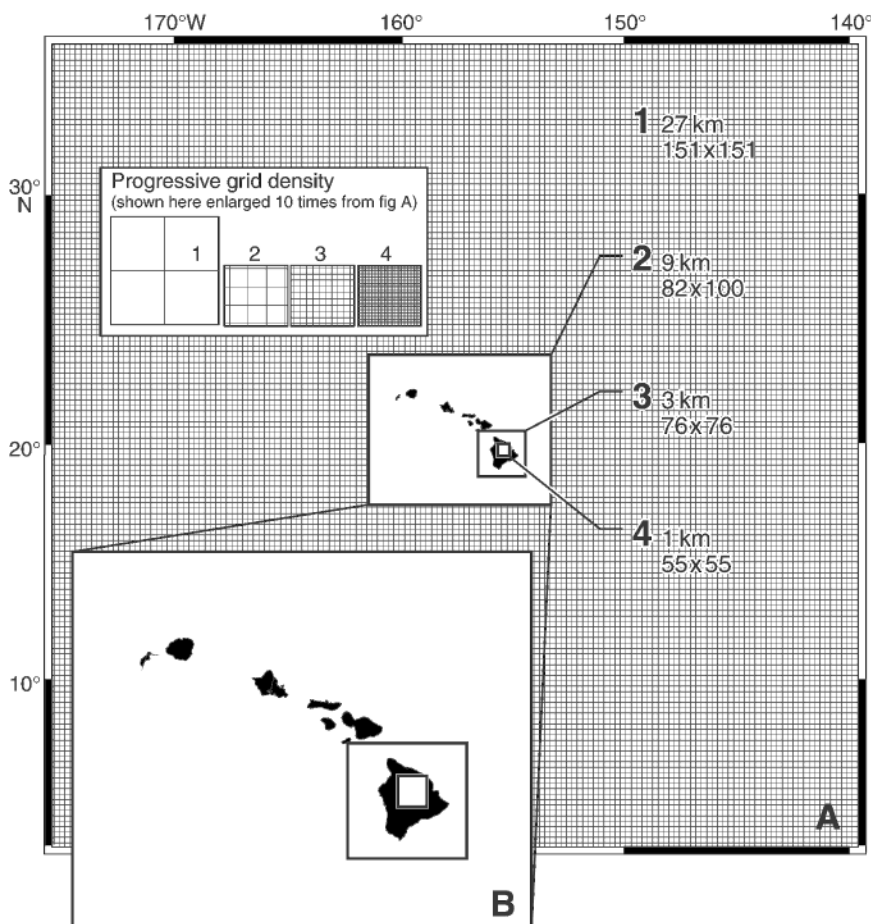


FIG. 7. Schematic showing domains of four MM5 nested grids used in daily simulations for Mauna Kea Observatories.

10 min, and in some cases more frequently. The CFHT tower is located on the eastern edge of the summit area at an altitude of ~4195 m (~13,765 ft; ~615 hPa), and it provides the most representative wind measurements, especially during persistent easterly trade wind periods. Analysis of 10 yr of temperature observations from the UKIRT weather tower (~4203 m; ~13,790 ft) reveals characteristics useful in refining summit temperature prediction. The other towers are located farther west and at slightly lower altitude, and help to describe temperature and wind variations across the summit area. Similar data are collected at the Mauna Kea site of the Very Long Baseline Array (VLBA), which is located on the southern slope at an altitude of ~3600 m (~12,000 ft or 650 hPa). Additionally, Web cameras provide outdoor views updated every 5–10 min from the CFHT, UKIRT, JCMT, and the VLBA sites.

The Caltech Submillimeter (CSO) measures atmospheric opacity (τ) above Mauna Kea at 225 GHz. Integrated precipitable water vapor (IPWV) is approximately related to τ by the relationship, IPWV (in mm) $\sim \tau/0.05$, based upon Chamberlin and Bally (1994). The CSO τ measurement provides the only “ground truth” for IPWV above Mauna Kea, at this time. A global positioning system (GPS) receiver has been installed at the summit and IPWV data (Businger et al. 1996) from this and other receivers located in Hawaii are processed in real time at the University of Hawaii at Manoa.

Surface observations are also available from Mauna Loa Observatory (MLO), a National Oceanic and Atmospheric Administration (NOAA) climate monitoring station located at an altitude of ~3,400 m (~11,000 ft) on the northern slope of Mauna Loa, about 35 km south of the Mauna Kea summit. A Web camera pointed north toward Mauna Kea monitors upslope cloud development and the strength of the inversion, while an upward-pointing camera monitors cirrus over the Island of Hawaii.

The MKWC will benefit from installations of new instrumentation on the Island of Hawaii summits that are planned for the near future. These include a wide-angle 10- μm camera to monitor cirrus, a small telescope system designed to monitor seeing conditions, and additional temperature sensors at several altitudes on existing instrumented towers planned for Mauna Kea. An ultraviolet light detection and ranging (LIDAR) for measuring vertical wind profiles and turbulence will be installed in 2001 at the Mauna Loa Observatory as a demonstration for a future spaceborne instrument.

Satellite data represent a valuable tool both for Mauna Kea forecasters and for an astronomer

conducting an observation run. The data are used primarily for nowcasts and short-term forecasts of storm systems, cloud coverage, summit fog, upper-tropospheric winds, and precipitable water. *Geostationary Operational Environmental Satellite-10 (GOES-10)* and the Geostationary Meteorological Satellite (GMS) imagery tailored to the needs of Mauna Kea astronomers are produced and disseminated via the MKWC Web site. High-resolution *GOES-10* (4 km) infrared satellite data are custom enhanced to differentiate between clouds above and below the mountain summit through the relationship between cloud-top temperatures and altitude (Fig. 3b), allowing astronomers to discern the presence of overhead cloudiness. Infrared imagery is used in concert with high resolution 1-km resolution visible imagery, 8-km resolution 6.7- μm water vapor channel imagery (all shown in Fig. 3), and summit in situ observations to generate the short-term forecasts and nowcasts.

Forecasting conventional meteorological variables.

Summit temperature undergoes a diurnal cycle forced by insolation. The amplitude weakens as summit winds strengthen and/or overhead clouds or summit fog thicken. Variability is caused by transient synoptic-scale systems in the midtroposphere, particularly cold-core lows, which occur with greater frequency in winter than in summer. MM5 captures both the diurnal cycle and transient systems for forecasts within 24 h. AVN and MRF provide guidance beyond 24 h for temperature changes resulting from transient midtropospheric systems. Even though global models do not include terrain, forecasts of the free atmosphere temperature at summit altitude are pertinent since the summit intercepts free atmosphere air at night. This point is confirmed by the fact that summit temperature typically changes by no more than 1°C between sunset and sunrise (Morrison et al. 1973). However, the change from one night to the next is often as much as 5°C. Mauna Kea’s summit is often near the freezing level and thus has an annual mean summit temperature of near 0°C, with extremes near -10°C and +12°C.

The overnight summit area (~615–625 hPa) temperature is usually 1°–2°C colder than the 600-hPa temperature projected near the Island of Hawaii by the AVN model. This discrepancy increases as summit winds strengthen, presumably mixing colder air from above down to the summit area. Unlike the AVN prognoses, the MM5 summit temperature forecast captures the diurnal cycle and assists in issuing forecasts of daytime maxima. MM5 underestimates the true elevation of the summit by ~200 m and has a con-

sistent warm bias of $\sim 2^{\circ}$ – 3°C that is easily taken into consideration.

Figure 8 depicts a year of MKWC summit temperature forecasts for 1200 UTC (0200 HST). Temperatures during this year range between -7° and 6°C . Since the rms error is less than the desired $\sim 1^{\circ}\text{C}$ upper limit for the temperature difference between the mirror and ambient error, MKWC summit temperature forecasts are of significant operational benefit. This benefit is especially noticeable for newer telescopes such as Gemini and Subaru. Most of the Mauna Kea telescopes are equipped with cooling systems for their primary mirrors, and for their telescope structures and enclosures. The temperature control setting for the cooling systems of Subaru and Gemini have been based on the MKWC forecast for Mauna Kea Observatories since May 2000. A significant improvement in image quality with the Subaru telescope has resulted.

The Mauna Kea summit experiences prevailing easterly trade winds emanating from a persistent subtropical ridge located to the northeast. The synoptic-scale ridge is well represented in the global models. The MM5 24-h summit wind forecasts account for the terrain of Mauna Kea and are therefore more accurate and physically realistic than the AVN forecasts, since the terrain enhances and sometimes doubles the free atmosphere wind speed. Beyond 24 h, the AVN 600-hPa wind prognoses provide useful estimates of the lower end of the speed range and wind direction, especially during the persistent easterly trades. Summit wind forecasts are combined with temperature forecasts to issue advisories for wind

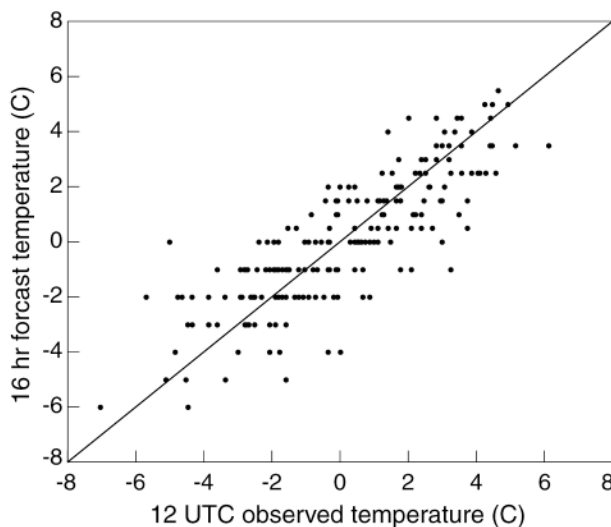


FIG. 8. Observed vs 16-h MKWC forecast summit temperature valid at 1200 UTC on nights from 1 Sep 1999 to 31 Aug 2000. The rms error = 0.634°C .

chill hazard. Forecasts of the vertical wind profile are a component of the seeing forecast methodology, described below.

Summit wind forecasts are sufficiently reliable to benefit telescope operations, largely due to the guidance from MM5. For example, the northeast wind of 18 kt observed at the Mauna Kea summit compares well with the MM5 forecast of northeasterly near 20 kt valid at the same time (Fig. 9a). Note the deflection of the wind by Mauna Kea in the MM5 simulation. Observed wind speeds generally fall within the MKWC forecast wind speed range, with a slight tendency to underforecast the strength of the winds overall (Fig. 10).

The water vapor channel temperature and MM5 forecasts of summit-upward IPWV are usually well correlated, and trends in water vapor can be forecast using MM5 guidance (cf. Figs. 9b and 9c). However, absolute magnitudes of IPWV above the summit are more challenging to predict. *GOES-10* $6.7\text{-}\mu\text{m}$ imagery and the CSO 225-GHz opacity are the tools used to observe and nowcast IPWV above Mauna Kea. The MM5 model output is used for 24-h forecasts. IPWV guidance above 625 hPa, calculated from global model output, is not very precise due to a lack of vertical resolution, the small magnitude of the quantity, and the lack of terrain effects in the model. Since most of the precipitable water is contained in the first 1 km above Mauna Kea, 600- and 500-hPa relative humidity prognoses provide useful general guidance. Preliminary analysis shows that the rms error in the IPWV forecasts is approximately 2.5 mm (not shown). Mauna Kea telescopes viewing in the infrared benefit from advance knowledge of IPWV to within ~ 1.0 mm at the dry end of the range. Since the forecast errors increase with increasing moisture, the preliminary results are promising; nevertheless, more research is needed to improve MKWC moisture forecasts.

Upper-level troughs cause plumes of mid- and upper-level clouds above Mauna Kea that emanate from enhanced convection along the intertropical convergence zone (ITCZ) and prevent observing for several days (Knabb and Fuelberg 2000; Iskenderian 1995; McGuirk et al. 1987; Fig. 3a). Plume events are more common over the northeastern Pacific than in any other region of the globe. They most frequently impact Hawaii between October and May when midlatitude troughs are most likely to penetrate into tropical latitudes and bring southwesterly flow aloft over Hawaii. Cirrus cloud cover can occur throughout the year as a result of blowoff from deep convection. Tropical upper-tropospheric troughs (TUTTs;

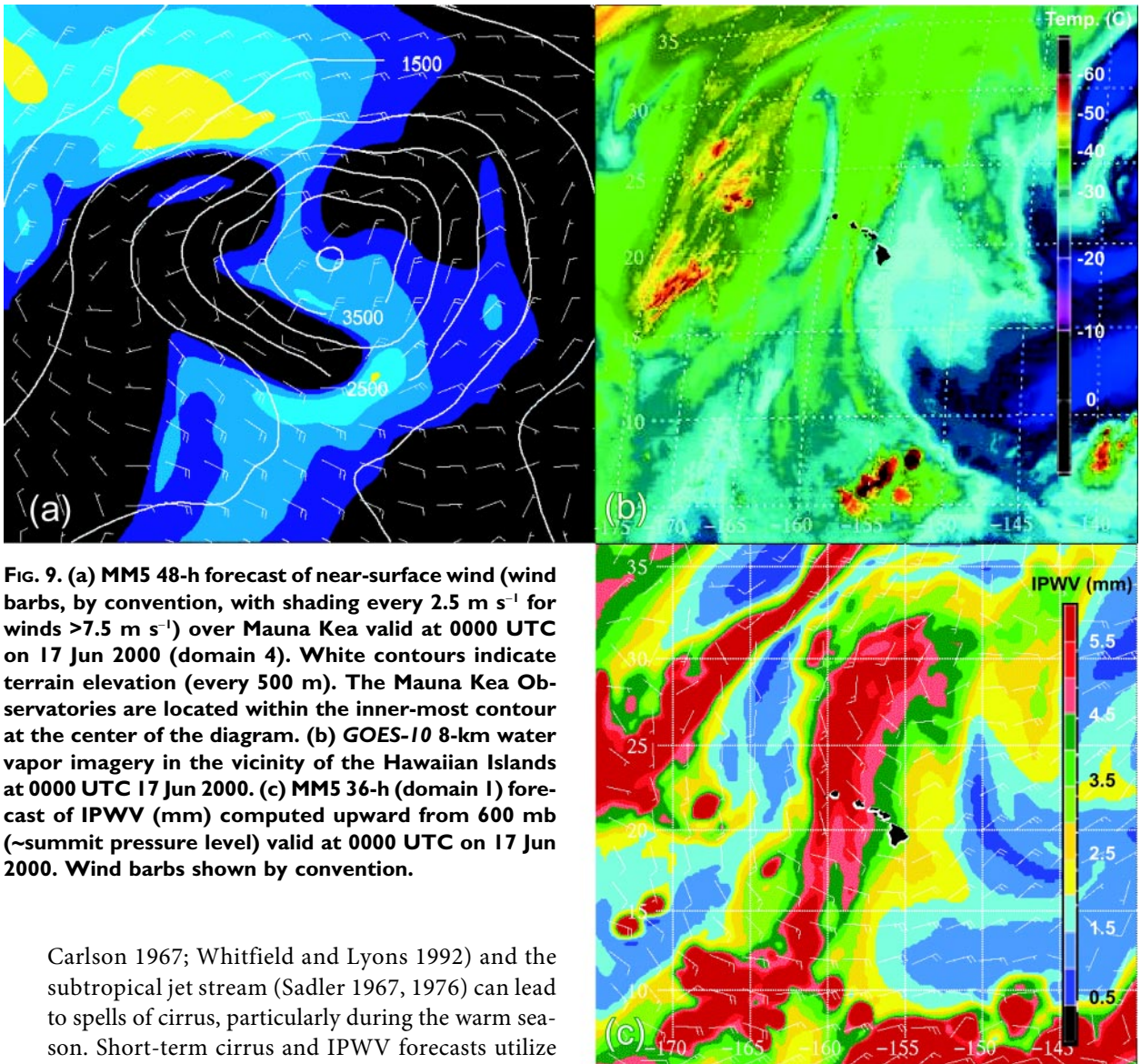


FIG. 9. (a) MM5 48-h forecast of near-surface wind (wind barbs, by convention, with shading every 2.5 m s^{-1} for winds $>7.5 \text{ m s}^{-1}$) over Mauna Kea valid at 0000 UTC on 17 Jun 2000 (domain 4). White contours indicate terrain elevation (every 500 m). The Mauna Kea Observatories are located within the inner-most contour at the center of the diagram. (b) GOES-10 8-km water vapor imagery in the vicinity of the Hawaiian Islands at 0000 UTC 17 Jun 2000. (c) MM5 36-h (domain I) forecast of IPWV (mm) computed upward from 600 mb (~summit pressure level) valid at 0000 UTC on 17 Jun 2000. Wind barbs shown by convention.

Carlson 1967; Whitfield and Lyons 1992) and the subtropical jet stream (Sadler 1967, 1976) can lead to spells of cirrus, particularly during the warm season. Short-term cirrus and IPWV forecasts utilize qualitative aspects of the approach of Erasmus and Peterson (1997), whereby the direction and speed of geostationary satellite image features are extrapolated using model output winds above the forecast site to estimate future values. While this method of forecasting is often skillful out to 24–36 h, it does not account for the dissipation or generation of cirrus. AVN model relative humidity prognoses provide guidance; regions exceeding $\sim 70\%$ humidity at levels above the summit up to about 200 hPa are favorable for cirrus formation. Density of cloudiness is characterized as mostly thin, a mix of thin and opaque, or mostly opaque. MM5 cloud products are under development to more explicitly forecast cloud coverage and density.

Weather systems that disrupt the prevailing trade wind inversion enhance convective cloud development and the probability of summit fog. Common

causes of fog are nearby weak tropical disturbances, a northward displacement of the ITCZ, and upper-level lows and troughs. Conversely, strong trade winds can orographically force low-level clouds upslope and cause summit fog, particularly in the absence of a strong trade wind inversion. Fortunately for the observatories, summit fog is far more common during daytime hours, when daytime heating erodes the inversion and supports upslope flow, than at night when downslope flow dominates (Morrison et al. 1973; Erasmus 1986).

Predictions of freezing level are used to assess the potential of icing and its impact on summit road access. Snow forecasts are based upon atmospheric stability, the absence of a lower-tropospheric inversion, and lower-tropospheric moisture advection, usually

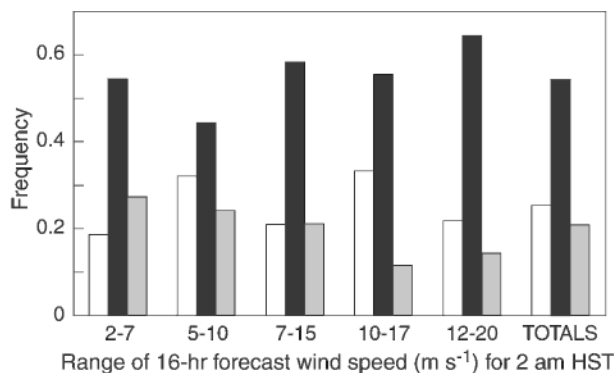


FIG. 10. Histogram of frequency distribution of forecast vs observed wind speed at the Mauna Kea summit for the period 1 Sep 1999–31 Aug 2000. Black bar indicates observed wind speed was in the forecast range; white and gray bars indicate under- and overforecast winds, respectively.

with a southerly component. Summit winds are incorporated to forecast blowing and/or drifting snow. Forecasts of cloud cover and density, and precipitation associated with tropical plumes and storm systems are labor intensive to verify and are the subject of ongoing verification efforts.

FORECASTING OBSERVING QUALITY—SEEING PARAMETERS.

Clear-air turbulence in both the free atmosphere and in the summit boundary layer can cause phase distortions to incoming electromagnetic wave fronts, resulting in motion, intensity fluctuations (scintillation), and blurring of images obtained by ground-based telescopes. Astronomical parameters that quantify these effects are generically referred to as seeing. However, seeing more specifically has the units of arc seconds and describes the angle occupied by the star image, at the full-width and half-maximum of its intensity profile, as viewed from a specific point in the atmosphere (Coulman et al. 1986). Seeing improves or degrades with changes in the vertical location and strength of turbulence as quantified by profiles of the refractive index structure function C_n^2 (Hill 1989; Nastrom and Eaton 1993). The C_n^2 fluctuations usually occur at scales that are too small for routine direct measurement, but they can be parameterized from vertical gradients in wind, temperature, and moisture. Seeing at a particular wavelength is then calculated by vertically integrating the C_n^2 profile. Since seeing at Mauna Kea varies significantly from one night to the next, or even within one night, as a result of changing synoptic and mesoscale flow patterns, accurate seeing forecasts enable telescopes to take best advantage of conditions that are favorable for a particular type of observation.

An MM5 postprocessing algorithm calculates C_n^2 and seeing, which in turn provide valuable guidance to Mauna

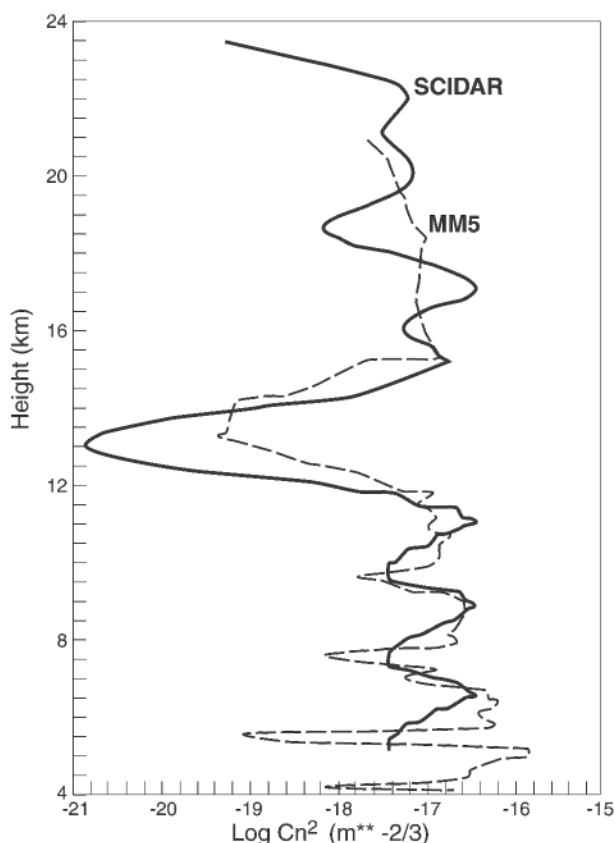


FIG. 11. Comparison of C_n^2 profiles obtained by SCIDAR observations (solid) and calculated from MM5 forecast wind and temperature profiles (dashed) for 1300 UTC on 13 Nov 1987.

Kea forecasters and astronomers regarding expected changes in observing quality. MM5 output temperature and wind profiles at each grid point are processed individually. The algorithm involves three major steps to arrive at a seeing forecast. First, the mixing length in each vertical layer of a profile is parameterized through application of the Dewan method in which the mixing length is determined by the strength of the vertical wind shear and the height of the layer relative to the tropopause (Roadcap and Morgenstern 1995). Next, profiles of C_n^2 are calculated from the profiles of temperature, wind, and mixing length. Strong turbulence (greater C_n^2) occurs in layers containing strong vertical temperature gradients and/or strong vertical wind shear.

Finally, the total impact of turbulence on ground-based observing is estimated by integrating the C_n^2 profiles to determine the seeing (Coulman et al. 1986; Bougeault et al. 1995). The 550-nm wavelength is used to provide a forecast of seeing at optical wavelengths. The viability of the seeing forecast methodology was tested in case study mode, using Scintillation Detection and Ranging (SCIDAR) observations that were obtained as part of a

field effort in 1987 to examine contributions to seeing conditions over Mauna Kea (Roddier et al. 1990). A comparison of C_n^2 profiles obtained by SCIDAR observations and from MM5 shows good agreement (Fig. 11).

Graphical depictions of the MM5-derived vertical profiles of C_n^2 and seeing above the Mauna Kea summit at 3-h intervals are provided as part of the daily Mauna Kea forecasts (Fig. 12). Explicit seeing forecasts using MM5 are available out to 24 h at this time. Subjective seeing forecasts are issued up to one week in advance using the AVN and MRF temperature and wind profiles as guidance. These forecasts rely upon an understanding of the effects of certain features in the vertical profile, such as strong vertical wind shear, on seeing. Recently initiated operational seeing forecasts compare favorably with actual astronomical images from telescopes on Mauna Kea.

SUMMARY AND FUTURE RESEARCH. A fortunate combination of geographic location, topography, and meteorological conditions makes Mauna Kea perhaps the best site on Earth for astronomy. Because of its remote subtropical location and summit altitude of more than 4 km, the prevailing clear, dry atmosphere above Mauna Kea provides optimum conditions for observing in the optical and infrared wavelengths. Recent innovations in telescope instrumentation and scheduling, together with progress in mesoscale numerical weather prediction, have made an imperative case for investment in custom weather forecast support for Mauna Kea. The Mauna Kea Weather Center (MKWC) is a new research program at the University of Hawaii at Manoa that is dedicated to providing custom forecast support to optimize astronomical operations on Mauna Kea.

Astronomical observing quality at the summit varies significantly even during prevalent fair weather conditions because of the impact of clear-air turbulence and density gradients on image motion and blurring. The astronomical parameter that quantifies these effects is generally referred to as seeing. Changes in seeing with time are explicitly derived from MM5 forecasted temperature and wind profiles. A factor that influences astronomical operations is the total or integrated precipitable water vapor above the summit, since it attenuates the radiative flux received from astronomical objects observed at infrared wavelengths. Satellite data are used in short-term forecasts of precipitable water. MM5 forecasts capture synoptic-scale changes in water vapor as well as the typical diurnal cycle of precipitable water driven by moist upslope flow during daytime hours. Summit temperature is another important forecast variable, since telescope mirrors and enclosures must be kept close to the ambient air temperature to optimize image quality. MKWC forecasts of overnight summit temperature are used to slowly warm or cool

mirrors, and are particularly important when abrupt air temperature changes are anticipated.

Adverse weather conditions can disrupt telescope operations and occasionally result in closure of summit facilities. Plumes of mid- and upper-tropospheric clouds, high winds, frozen precipitation, fog associated with tropical and midlatitude cyclones, and troughs aloft are a special focus of the forecast center. Forecast and data dissemination is accomplished through the Internet, with animations of satellite and model output available at the MKWC Web site (hokukea.soest.hawaii.edu). Access to MKWC products enables the telescope staff to optimize their strategy prior to and during each observing run and to mitigate the effects of weather hazards.

A primary objective of the operational mesoscale numerical modeling effort at the MKWC has been the development of seeing forecasts. The simulation of astronomical parameters is a unique research problem that has seen limited attention in the literature to date. Sensitivity studies using MM5 have been undertaken to determine an optimal model configuration to simulate the high-resolution vertical temperature and wind profiles needed to accurately compute required astronomical parameters. Continued progress in numerical prediction of seeing would benefit greatly from the availability of observational data on the vertical structure of the atmosphere over Mauna Kea in concert with observations of astronomical parameters. To that end, a field campaign is being developed to measure seeing and profiles of wind, temperature, and C_n^2 over Mauna Kea. The goal of the field campaign is to obtain a better understanding of the relationship between various weather patterns and seeing.

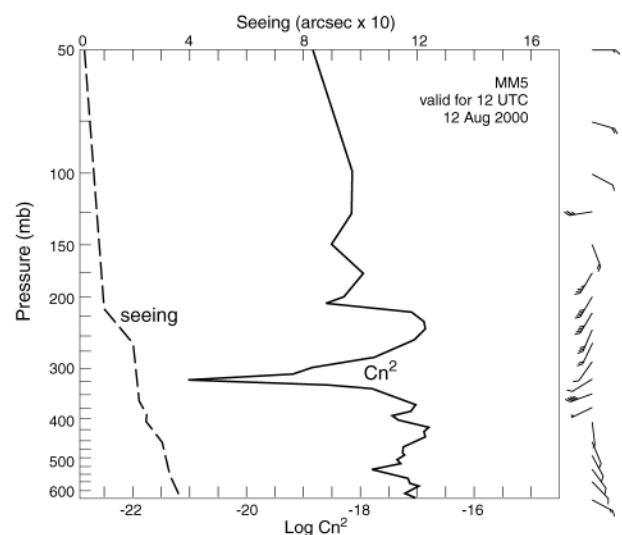


FIG. 12. The C_n^2 and seeing profiles derived from MM5 output for a day with very good seeing quality, valid at 1200 UTC on 2 Aug 2000.

Assessment of the skill of customized forecasts is an important goal of the MKWC because it provides necessary feedback to forecasters regarding progress. Obtaining forecast verifications represents an extensive data collection and processing effort that is undertaken on an ongoing basis. It is anticipated that a general increase in forecast skill and precision will accompany improvements in the accuracy of MM5 simulations. Improvements in the implementation of MM5 are a high priority for the project and require a significant investment in human and computational resources. Improvements will occur as a result of data assimilation over the data-sparse central Pacific (e.g., satellite-derived moisture and winds and LIDAR-derived wind, temperature, and moisture profiles) and changes in the configuration of the MM5 model. Model runs with and without assimilated data or configuration changes will be compared with observational data to assess the impact of the changes. Comprehensive verification of MM5 output and implementation of data assimilation are significant ongoing research efforts at MKWC.

Growing archives of daily MM5 output, satellite data, and astronomical observations afford a special opportunity to study in detail several aspects of tropical meteorology that affect Mauna Kea. Among the issues being addressed are the incomplete understanding of tropical-extratropical interactions, the effects of mesoscale processes in a region of complex terrain, and the dependence of seeing forecasts on model resolution. MM5 sensitivity simulations for particular storm events are planned in an effort to improve MM5's ability to simulate storm structure and evolution. Results from these investigations in turn will lead to improved MKWC forecasts of hazardous weather events. Two primary candidates for study are kona lows and tropical cyclones, both of which pose a wide range of hazards to Mauna Kea.

ACKNOWLEDGMENTS. We are grateful to Richard Knabb for his instrumental role in the development stage of the MKWC and contributions to and review of the manuscript. We wish to acknowledge the support and collaboration provided by the NWSFO-HFO. Particular thanks go to Paul Jendrowski and Jim Weyman for their significant contribution to the success of this project. We are grateful to George Jumper (AFRL) for information on calculation of seeing variables. We are grateful for the constructive comments of Thomas Fahey and two anonymous reviewers. The National Astronomical Observatory of Japan provides computer resources, located at the Subaru Telescope facility in Hilo, Hawaii, for the MM5 simulations. This research was supported in part by funding provided

by the Gemini Observatory, which is operated by the Association of Universities for Research in Astronomy, Inc., under a cooperative agreement with the NSF on behalf of the Gemini partnership: the National Science Foundation (United States), the Particle Physics and Astronomy Research Council (United Kingdom), the National Research Council (Canada), CONICYT (Chile), the Australian Research Council (Australia), CNPq (Brazil), and CONICET (Argentina).

REFERENCES

- Birkenheuer, D., 1999: The effect of using digital satellite imagery in the LAPS moisture analysis. *Wea. Forecasting*, **14**, 782–788.
- Bougeault, P., C. De Hui, B. Fleury, and J. Laurent, 1995: Investigation of seeing by means of an atmospheric mesoscale numerical simulation. *Appl. Opt.*, **34**, 3481–3488.
- Businger, S., and Coauthors, 1996: The promise of GPS in atmospheric monitoring. *Bull. Amer. Meteor. Soc.*, **77**, 5–18.
- , T. Birchard Jr., K. R. Kodama, P. A. Jendrowski, and J.-J. Wang, 1998: A bow echo and severe weather associated with a kona low in Hawaii. *Wea. Forecasting*, **13**, 576–591.
- Carlson, T. N., 1967: Structure of a steady state cold low. *Mon. Wea. Rev.*, **95**, 763–777.
- Chamberlin, R. A., and J. Bally, 1994: 255-GHz atmospheric opacity of the South Pole sky derived from continual radiometric measurements of the sky-brightness temperature. *Appl. Opt.*, **33**, 1095–1099.
- Coulman, C. E., J.-C. Andre, P. Lacarrere, and P. R. Gillingham, 1986: The observation, calculation, and possible forecasting of astronomical seeing. *Publ. Astron. Soc. Pac.*, **98**, 376–387.
- Erasmus, D. A., 1986: Meteorological conditions affecting observing quality on Mauna Kea. *Publ. Astron. Soc. Pac.*, **98**, 254–259.
- , and R. Peterson, 1997: The feasibility of forecasting cirrus cloud cover and water vapor above telescope sites in northern Chile. *Publ. Astron. Soc. Pac.*, **109**, 208–214.
- Grell, G. A., 1993: Prognostic evaluation of assumptions used by cumulus parameterizations. *Mon. Wea. Rev.*, **121**, 764–787.
- , J. Dudhia, and D. R. Stauffer, 1995: A description of the Fifth-Generation Penn State/NCAR Mesoscale Model (MM5). NCAR/TN-398+STR, National Center for Atmospheric Research, Boulder, CO, 122 pp.
- Grinding, C. M., 1992: Temporal variability of the trade wind inversion: Measured with a boundary

- layer vertical profiler. M.S. thesis, Dept. of Meteorology, University of Hawaii at Manoa, 93 pp. [Available from Dept. of Meteorology, University of Hawaii at Manoa, 2525 Correa Rd., Honolulu, HI 96822.]
- Hill, R. J., 1989: Structure functions and spectra of scalar quantities in the inertial-convective and viscous-convective ranges of turbulence. *J. Atmos. Sci.*, **46**, 2245–2251.
- Iskenderian, H., 1995: A 10-year climatology of Northern Hemisphere tropical cloud plumes and their composite flow patterns. *J. Climate*, **8**, 1630–1637.
- Jumper, G. Y., and R. R. Beland, 2000: Progress in the understanding and modeling of atmospheric optical turbulence. *Proc. 31st Plasmadynamics and Lasers Conf.*, Denver, CO, American Institute of Aeronautics and Astronautics, 1609–1616.
- Knabb, R. D., and H. E. Fuelberg, 2000: Three-dimensional structure, scale interactions, and moisture transport in three types of tropical cloud plumes. Preprints, *24th Conf. on Hurricanes and Tropical Meteorology*, Fort Lauderdale, FL, Amer. Meteor. Soc., 171–172.
- Kodama, K. R., and S. Businger, 1998: A brief overview of weather and forecasting in the Pacific region of the National Weather Service. *Wea. Forecasting*, **13**, 523–546.
- Masciadri, E., J. Vernin, and P. Bougeault, 1998: 3D mapping of optical turbulence using an atmospheric numerical model. I: A useful tool for ground-based astronomy. *Astron. Astrophys.*, **15**, 37–58.
- McGuirk, J. P., A. H. Thompson, and N. R. Smith, 1987: Moisture bursts over the tropical Pacific Ocean. *Mon. Wea. Rev.*, **115**, 787–798.
- Mello, C., 1998: Wind storms associated with an enhanced Hawaiian high in winter. M.S. thesis, Dept. of Meteorology, University of Hawaii at Manoa, 59 pp. [Available from Dept. of Meteorology, University of Hawaii at Manoa, 2525 Correa Rd., Honolulu, HI 96822.]
- Michalakes, J., 1998: Design of a next-generation weather research and forecast model. *Proc. Eighth Workshop on the Use of Parallel Processors in Meteorology*, Reading, United Kingdom, European Centre for Medium-Range Weather Forecasts, 269–276.
- Morrison, D., R. E. Murphy, D. P. Cruikshank, W. M. Sinton, and T. Z. Martin, 1973: Evaluation of Mauna Kea, Hawaii, as an observatory site. *Publ. Astron. Soc. Pac.*, **85**, 255–267.
- Morrison, I., and S. Businger, 2001: The synoptic structure and evolution of a kona low. *Wea. Forecasting*, **16**, 81–98.
- Nastrom, G. D., and F. D. Eaton, 1993: The coupling of gravity waves and turbulence at White Sands, New Mexico, from VHF radar observations. *J. Appl. Meteor.*, **32**, 81–87.
- Roadcap, J. R., and C. D. Morgenstern, 1995: Comparison of observed and modeled isoplanatic angles using synoptic weather data. *Proc. Beam Control, Diagnostics, Standards, and Propagation*, San Jose, CA, International Society for Optical Engineering, 41–50.
- Roddier, F., and Coauthors, 1990: Seeing at Mauna Kea: A joint UH–UN–NOAO–CFHT study. *Proc. Advanced Technology Optical Telescopes IV*, Bellingham, WA, International Society for Optical Engineering, 485–491.
- Sadler, J. C., 1967: The tropical upper tropospheric trough as a secondary source of typhoons and a primary source of tradewind disturbances. *Rep. No. 67-12*, Hawaii Institute of Geophysics, University of Hawaii, Honolulu, 96822, 103 pp.
- , 1976: A role of the Tropical Upper Tropospheric Trough in early season typhoon development. *Mon. Wea. Rev.*, **104**, 1266–1278.
- Whitfield, M. B., and S. W. Lyons, 1992: An upper-tropospheric low over Texas during summer. *Wea. and Forecasting*, **7**, 89–106.
- Worthley, L. E., 1967: Weather phenomena in Hawaii. Part I. Synoptic climatology of Hawaii. Hawaii Institute of Geophysics, University of Hawaii, 40 pp. [Available from Dept. of Meteorology, University of Hawaii, 2525 Correa Rd., Honolulu, HI 96822.]